Ferromagnetic Interactions in the $Mn(N_3)_4[Ni(en)_2(NO_2)]_2$ Trinuclear Compound. Crystal Structure and Physical Properties

T. M. Rajendiran,[†] Corine Mathonière,[†] Stéphane Golhen,[‡] Lahcène Ouahab,[‡] and Olivier Kahn*,[†]

Laboratoire des Sciences Moléculaires, Institut de Chimie de la Matière Condensée de Bordeaux, UPR CNRS No. 9048, 33608 Pessac, France, and Laboratoire de Chimie du Solide et Inorganique Moléculaire, UMR No. 6511, Université de Rennes I, 35042 Rennes, France

Received July 8, 1997

The goal of this work was to design a ferromagnetically coupled $Mn^{2+}Ni^{2+}$ species. For this, we attempted to combine nitro−nitrito and end-on azido bridges which are both known to be ferromagnetic couplers. This has led us to the compound of formula $Mn(N_3)_4[Ni(en)_2NO_2]_2$ (en = ethylenediamine). The crystal structure has been solved at room temperature. The compound crystallizes in the monoclinic system, space group *C*2, with $a = 12.631(14)$ Å, $b = 15.636(2)$ Å, $c = 13.43(2)$ Å, $\beta = 90.14(6)°$, and $Z = 4$. The structure consists of two very similar but crystallographically independent neutral trinuclear units with a $MnNi_2$ isoceles triangular shape. The Mn and Ni atoms are doubly bridged by an end-on azido and a nitro−nitrito (with respect to Ni and Mn, respectively) group. Both the temperature dependence of the magnetic susceptibility and the field dependence of the magnetization at 2 K have been investigated and have revealed $Mn^{2+}-Ni^{2+}$ ferromagnetic interactions, which give rise to an $S = {}^9/_2$ ground state for the triad. The quantitative interpretation of these magnetic properties has given an interaction parameter J between Mn^{2+} and Ni^{2+} ions equal to 1.4(1) cm^{-1} ($\boldsymbol{H} = -J\mathbf{S_{Mn}}\cdot(\mathbf{S_{Ni1}} + \mathbf{S_{Ni2}})$). The electronic absorption spectrum has been recorded at various temperatures down to 20 K and interpreted.

Introduction

For quite a few years we have been interested in the topologies leading to ferromagnetic interactions between transition metal ions.[1] To control the nature of the interaction between magnetic ions in a polynuclear compound, we can utilize at least two factors, namely (i) the relative symmetries of the magnetic orbitals, and (ii) the nature of the bridging network. Concerning the former factor, it is now well established that the strict orthogonality of the magnetic orbitals stabilizes the high-spin state, and many applications of this concept have been reported.[2−6] Concerning the latter factor, it has been experimentally demonstrated and sometimes theoretically rationalized that some bridges may be considered as ferromagnetic couplers. Probably, the best known example is the end-on azido bridge.[7−10] To the best of our knowledge, in all cases where the metal ions are only bridged by end-on azido groups, the parallel spin state is the ground state. On the other hand, the situation may be different when the bridging network involves both an end-on azido bridge and another type of bridge.[11,12]

Very recently we reported on a $Mn^{2+}Ni^{2+}$ bimetallic chain compound in which the Mn^{2+} and Ni^{2+} ions were ferromagnetically coupled through NO_2^- bridges.[13] The bridging network was

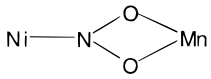

with a nitro coordination with respect to Ni^{2+} and a bidentate nitrito coordination with respect to Mn^{2+}.

Bearing in mind that (i) the end-on azido bridge is a very efficient ferromagnetic coupler and (ii) the nitro−nitrito bridge may be also a ferromagnetic coupler, at least between Ni^{2+} and Mn^{2+} ions, we attempted to combine these two bridges and to construct a μ-1,1-azido−μ-nitro−nitrito−nickel(II)−manganese(II) species. This led us to the trinuclear compound $Mn(N_3)_4[Ni(en)_2NO_2]_2$, which is the subject of this paper.

We will successively describe the synthesis, the crystal structure, the magnetic and EPR properties, and the optical properties of $Mn(N_3)_4[Ni(en)_2NO_2]_2$.

Experimental Section

Synthesis. The starting material $Ni(en)_2(NO_2)_2$ was synthesized as described previously.[14] $Mn(N_3)_4[Ni(en)_2NO_2]_2$ was synthesized as follows. To a purple solution of 0.540 g (2 mmol) of $Ni(en)_2(NO_2)_2$

[†] Institut de Chimie de la Matière Condensée de Bordeaux.
[‡] Université de Rennes I.

(1) Kahn, O. *Angew. Chem., Int. Ed. Engl.* **1985**, *24*, 834; *Struct. Bonding (Berlin)* **1987**, *68*, 89; *Adv. Inorg. Chem.* **1995**, *43*, 1789; *Molecular Magnetism*; VCH: New York, 1993.
(2) Kahn, O.; Galy, J.; Journaux, Y.; Morgenstern-Badarau, I. *J. Am. Chem. Soc.* **1982**, *104*, 2165.
(3) Gadet, V.; Mallah, T.; Castro, I.; Verdaguer, M. *J. Am. Chem. Soc.* **1992**, *114*, 9213.
(4) Lloret, F.; Ruiz, R.; Julve, M.; Faus, J.; Journaux, Y.; Castro, I.; Verdaguer, M. *Chem. Mater.* **1992**, *4*, 1150.
(5) Ohba, M.; Tamaki, H.; Matsumoto, N.; Okawa, H. *Inorg. Chem.* **1993**, *32*, 5385.
(6) Mitsumi, M.; Okawa, H.; Sakiyama, H.; Ohba, M.; Matsumoto, N.; Kurisaki, T.; Wakita, H. *J. Chem. Soc., Dalton Trans.* **1993**, 2991.
(7) Charlot, M. F.; Kahn, O.; Chaillet, M.; Larrieu, C. *J. Am. Chem. Soc.* **1986**, *108*, 2574.
(8) Ribas, J.; Monfort, M.; Diaz, C.; Bastos, C.; Solans, X. *Inorg. Chem.* **1994**, *33*, 484.
(9) Cortés, R.; Lezama, L.; Pisarro, J. L.; Solans, X.; Arriortua, M. I.; Rojo, T. *Angew. Chem., Int. Ed. Engl.* **1994**, *33*, 2488.
(10) Cortés, R.; Lezama, L.; Mautner, F. A.; Rojo, T. In *Molecule-Based Magnetic Materials*; Turnbull, M. M., Sugimoto, T., Thompson, L. K., Eds.; ACS Symposium Series 644; American Chemical Society: Washington, DC, 1996.
(11) Tandon, S. S.; Thompson, L. K.; Manuel, M. E.; Bridson, J. N. *Inorg. Chem.* **1994**, *33*, 5555.
(12) Thompson, L. K.; Tandon, S. *Comments Inorg. Chem.* **1996**, *18*, 125.
(13) Kahn, O.; Bakalbassis, E.; Mathonière, C.; Hagiwara, M.; Katsumata, K.; Ouahab, L. *Inorg. Chem.* **1997**, *36*, 1530.
(14) *Jikken Kagaku Koza*; Inokuchi, Ed.; Mazuren Co.: Tokyo, 1991.

S0020-1669(97)00853-7 CCC: $15.00
Published on Web 05/05/1998

Table 1. Crystallographic Data for $Mn(N_3)_4[Ni(en)_2(NO_2)]_2$

empirical formula	$C_8H_{32}N_{22}O_4MnNi_2$
a, Å	12.631(14)
b, Å	15.636(2)
c, Å	13.43(2)
β, deg	90.14(6)
V, Å^3	2652(4)
Z	4
fw	672.92
space group	$C2$ (No. 5)
T, K	293(2)
λ, Å	0.710 73
ρ_{calcd}, g cm^{-3}	1.685
μ, mm^{-1}	1.935
wR2[a]	0.0909 (for $F_o^2 \geq 2\sigma(F_o^2)$)
R1[b]	0.0355 (for $F_o^2 \geq 2.\sigma(F_o^2)$)

[a] $wR2 = [\sum[w(F_o^2 - F_c^2)^2]/\sum[w(F_o^2)2]]^{1/2}$. [b] $R1 = \sum||F_o| - |F_c||/\sum|F_o|$.

Table 2. Selected Bond Lengths (Å) for the Molecule $Mn(N_3)_2[Ni(NO_2)(N_3)]_2$ Shown in Figure 1[a]

Ni(1)−N(9)	2.088(7)	Mn(1)−O(1)	2.206(7)
Ni(1)−N(10)	2.089(7)	Mn(1)−N(4)	2.283(6)
Ni(1)−N(7)	2.104(7)	Mn(1)−N(4)^i	2.283(6)
Ni(1)−N(8)	2.104(6)	N(1)−N(2)	1.170(9)
Ni(1)−N(4)	2.132(7)	N(2)−N(3)	1.138(9)
Ni(1)−N(11)	2.214(7)	N(4)−N(5)	1.180(10)
Mn(1)−N(1)^i	2.174(7)	N(5)−N(6)	1.152(11)
Mn(1)−N(1)	2.174(7)	N(11)−O(2)	1.231(11)
Mn(1)−O(1)^i	2.206(7)	N(11)−O(1)	1.238(8)

[a] Superscript i corresponds to the symmetry transformation $-x$, y, $-z + 1$.

dissolved in 40 mL of methanol was added a solution of 0.197 g (1 mmol) of $MnCl_2 \cdot 6H_2O$ and 0.260 g (4 mmol) of NaN_3 dissolved in 20 mL of methanol. The resulting mixture was stirred for 1 h at room temperature and then reduced to 10 mL. Single crystals were obtained by slow evaporation. Anal. Calcd for $C_8H_{32}N_{22}O_4MnNi_2$: C, 14.27; H, 4.75; N, 45.81; Mn, 8.17; Ni, 17.45. Found: C, 13.91; H, 4.56; N, 45.44; Mn, 7.91; Ni, 17.23.

Crystallographic Data Collection and Structure Determination. A brown polyhedric crystal was mounted at the end of a glass fiber. Intensity data were obtained at room temperature on an Enraf-Nonius CAD4 diffractometer equipped with Mo Kα radiation (graphite monochromator), employing the $\theta-2\theta$ scan technique. A total of 3497 reflections ($1 \leq \theta \leq 28°$) were collected, yielding 3418 unique reflections ($R_{int} = 0.0273$), 2630 of them with $I > 2\sigma(I)$. The net intensity values of three standard reflections monitored after every 3600 s of X-ray exposure revealed no decay during the 52 h of exposure. Lorentz and polarization corrections[15] were applied as well as corrections for absorption effects. The latter were corrected by the semiempirical ψ-scan method[16] with minimum and maximum transmission coefficients of 0.9429 and 0.9999, respectively. The structure was solved by direct methods in SHELXS-86[17] and refined by full-matrix least-squares procedures based on F^2 in SHELXL-93.[18] Hydrogen atoms were located on the basis of geometrical considerations, and treated according to the riding model during refinement with isotropic displacement parameters corresponding to the heavy atoms they are linked to. All other atoms were assigned anisotropic displacement parameters. Crystallographic and refinement parameters are given in Table 1. Selected bond lengths and angles are given in Tables 2 and 3.

Magnetic Properties. These were carried out on powder samples with a Quantum Design MPMS-5S SQUID magnetometer working down to 2 K and up to 50 kOe. It was verified that the magnetic suceptibility did not depend on the magnitude of the applied magnetic field up to 2 kOe. The core diamagnetism was estimated as -360×10^{-6} emu mol^{-1}.

(15) *International Tables for X-ray Crystallography*; Kynoch Press: Birmingham, U.K., 1974; Vol. IV.
(16) North, A. C. T.; Philips, D. C.; Mathews, F. S. *Acta Crystallogr., Sect A*, **1968**, 351.
(17) Sheldrick, G. M. SHELXS-86: *Program for the solution of crystal structures*; University of Göttingen: Göttingen, Germany, 1986.
(18) Sheldrick, G. M. SHELXL 93: *Program for the refinement of crystal structures*; University of Göttingen: Göttingen, Germany, 1993.

Table 3. Selected Bond Angles (deg) for the Molecule $Mn(N_3)_2[Ni(NO_2)(N_3)]_2$ Shown in Figure 1[a]

N(9)−Ni(1)−N(10)	83.1(3)	N(9)−Ni(1)−N(7)	93.7(3)
N(10)−Ni(1)−N(7)	94.5(3)	N(9)−Ni(1)−N(8)	175.0(3)
N(10)−Ni(1)−N(8)	95.9(3)	N(7)−Ni(1)−N(8)	81.4(3)
N(9)−Ni(1)−N(4)	93.8(3)	N(10)−Ni(1)−N(4)	93.9(3)
N(7)−Ni(1)−N(4)	169.3(3)	N(8)−Ni(1)−N(4)	91.2(3)
N(9)−Ni(1)−N(11)	89.1(3)	N(10)−Ni(1)−N(11)	172.1(3)
N(7)−Ni(1)−N(11)	86.8(3)	N(8)−Ni(1)−N(11)	92.0(2)
N(4)−Ni(1)−N(11)	85.7(3)		
N(1)^i−Mn(1)−N(1)	93.7(4)	N(1)^i−Mn(1)−O(1)^i	95.9(3)
N(1)−Mn(1)−O(1)^i	90.2(3)	N(1)^i−Mn(1)−O(1)	90.2(3)
N(1)−Mn(1)−O(1)	95.9(3)	O(1)^i−Mn(1)−O(1)	171.2(3)
N(1)^i−Mn(1)−N(4)	173.7(4)	N(1)−Mn(1)−N(4)	90.4(2)
O(1)^i−Mn(1)−N(4)	88.8(3)	O(1)−Mn(1)−N(4)	84.7(2)
N(1)^i−Mn(1)−N(4)^i	90.4(2)	N(1)−Mn(1)−N(4)^i	173.7(4)
O(1)^i−Mn(1)−N(4)^i	84.7(2)	O(1)−Mn(1)−N(4)^i	88.8(3)
N(4)−Mn(1)−N(4)^i	85.9(3)		
N(3)−N(2)−N(1)	176.8(8)	Ni(1)−N(4)−Mn(1)	115.4(3)
N(6)−N(5)−N(4)	178.9(7)	O(2)−N(11)−Ni(1)	118.5(5)
O(2)−N(11)−O(1)	115.1(7)	N(11)−O(1)−Mn(1)	122.4(5)

[a] Superscript i corresponds to the symmetry transformation $-x$, y, $-z + 1$.

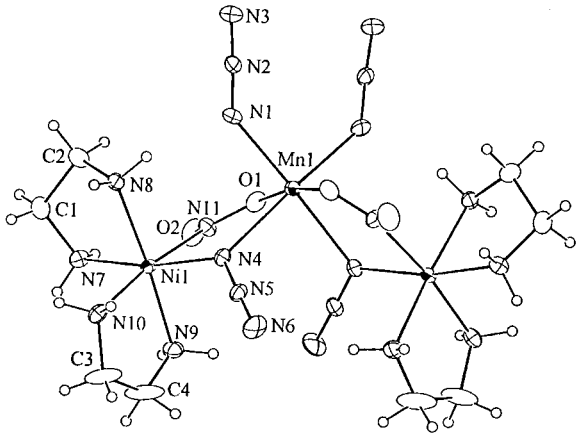

Figure 1. Structure of one of the two crystallographically independent molecules of $Mn(N_3)_4[Ni(en)_2NO_2]_2$.

Optical Spectra. These were recorded with a Cary 5E spectrophotometer equipped with a continuous-helium-flow cryostat provided by Oxford Instruments.

Description of the Structure

The structure consists of two almost identical but crystallographically independent trinuclear units, I and II; one of the units is shown in Figure 1. These units are neutral and rather well isolated from each other within the crystal lattice. Molecules I are organized in layers parallel to the *ab* plane, which alternate with layers of molecules II. For each molecule, I or II, one of the en ligands is orthogonal to the *bc* plane and the other is orthogonal to the *ab* plane. All the terminal azido groups are oriented along the *b*-axis direction.

The metal atoms of the trinuclear unit form an isoceles triangle with Mn- - -Ni and Ni-- -Ni separations equal to 3.733(3) and 6.479(7) Å, respectively, in one of the units (3.731(3) Å and 6.476(7) Å, respectively, in the other unit). The average values of the Ni−Mn−Ni and Mn−Ni−Ni angles are 120.4 and 29.8°, respectively. The manganese atom is located on a 2-fold symmetry axis in a distorded octahedral environment. It is surrounded by four nitrogen atoms from two terminal and two bridging azido groups and two oxygen atoms from bridging NO_2^- groups. The mean bond lengths are Mn−N(terminal) = 2.17 Å, Mn−N(bridging) = 2.27 Å, and Mn−O = 2.21 Å. Each nickel atom is also located in a distorted octahedral environment. It is surrounded by six nitrogen atoms, four from the two ethylenediamine ligands, one from the bridging azido group,

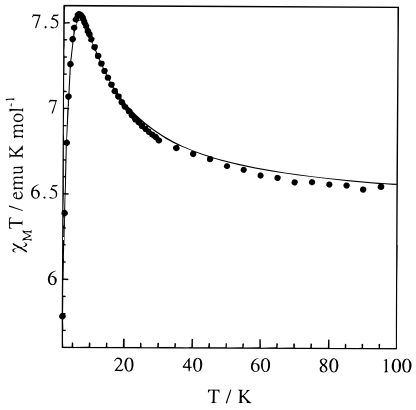

Figure 2. Experimental (•) and calculated (model I) (—) $\chi_M T$ versus T curves for $Mn(N_3)_4[Ni(en)_2NO_2]_2$.

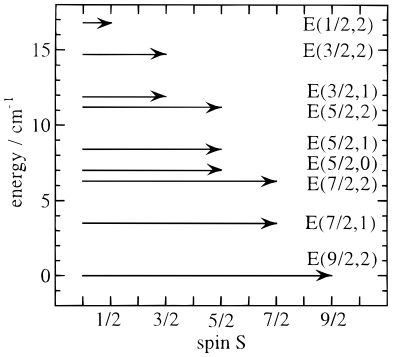

Figure 3. Spectrum of the low-lying states for $Mn(N_3)_4[Ni(en)_2NO_2]_2$, as deduced from the magnetic properties. Each state is represented by an arrow whose length is proportional to the spin value *S* associated to this state.

and the last one from the bridging NO_2^- group. The mean Ni−N bond lengths are Ni−N(en) = 2.10 Å, Ni−N(azido) = 2.13 Å, and Ni−N(nitro) = 2.22 Å.

The manganese and nickel atoms are doubly bridged by an end-on azido group and a nitro−nitrito group. As expected, both the terminal and bridging azido ligands are almost linear. The two N−O bond lengths of a nitro−nitrito bridge are very close to each other (mean value 1.23 Å), and the mean value of the ONO bond angle is 116°. The mean value of the bridging angle MnNNi involving the end-on azido bridge is also equal to 116°.

Magnetic Properties

The temperature (*T*) dependence of the molar magnetic susceptibility (χ_M) for $Mn(N_3)_4[Ni(en)_2(NO_2)]_2$ is shown in Figure 2 in the form of a $\chi_M T$ versus *T* plot; $\chi_M T$ is equal to 6.58 emu K mol^{-1} at room temperature, remains constant down to ca. 80 K, then increases as *T* is lowered further, presents a maximum around 6.5 K with $\chi_M T$ = 7.58 emu K mol^{-1}, and eventually falls. The $\chi_M T$ value at 2 K is 5.78 emu K mol^{-1}. This behavior reveals ferromagnetic Mn^{2+}−Ni^{2+} intramolecular interactions which give rise to an $S = {}^9/_2$ ground state. The magnetic behavior in the low-temperature range may be attributed to the local anisotropy of the Ni^{2+} ions and/or antiferromagnetic intermolecular interactions.

Let us interpret quantitatively the magnetic susceptibility data of Figure 2. For this, the spin Hamiltonian of the trinuclear species may be written as

$$\boldsymbol{H} = -J\mathbf{S_{Mn}}\cdot(\mathbf{S_{Ni1}} + \mathbf{S_{Ni2}}) + D_{Ni}(\mathbf{S_{z,Ni1}}^2 + \mathbf{S_{z,Ni2}}^2) + [g_{Mn}\mathbf{S_{Mn}} + g_{Ni}(\mathbf{S_{Ni1}} + \mathbf{S_{Ni2}})]\cdot\beta H \quad (1)$$

where the first term in the right-hand side describes the interaction between the Mn^{2+} and the two Ni^{2+} ions, the second term describes the local anisotropy of the Ni^{2+} ions supposed to be axial, and the third term describes the Zeeman perturbation under the effect of the applied magnetic field *H*. The local Zeeman factors g_{Mn} and g_{Ni} are considered to be isotropic. Let us note that in (1) the interaction between terminal Ni^{2+} ions and the anisotropic interactions are neglected.

Two approaches were used. The former (model I) consisted of deriving an analytical expression for χ_M in which only the zero-field splitting within the $S = {}^9/_2$ ground state was considered, with an axial zero-field-splitting parameter $D_{9/2}$. This expression was then modified to take into account the intermolecular interactions in the mean-field approximation. For this, the additional parameter zJ' was introduced. As could be anticipated, the *J*, zJ', and $D_{9/2}$ parameters were found to be correlated. Minimizing $R = \sum[(\chi_M T)^{exp} - (\chi_M T)^{cal}]^2/\sum[(\chi_M T)^{exp}]^2$ resulted in $J = 1.3$ cm^{-1}, $g_{Mn} = 1.97$, $g_{Ni} = 2.11$, $zJ' = -0.09$ cm^{-1}, and a negligibly small $D_{9/2}$ value.

In the latter approach (model II), the eigenfunctions and eigenvalues of (1) were determined by full diagonalization of the spin Hamiltonian $\boldsymbol{H}$, using the 54 microstates of the trinuclear system as a basis set. The first- and second-order Zeeman coefficients were then calculated and introduced in the Van Vleck equation. No set of *J*, D_{Ni}, g_{Mn}, and g_{Ni} parameters reproduces the experimental data down to 2 K in a fully satisfying manner. The experimental $\chi_M T$ values below 4 K are lower than the calculated ones, which suggests that very weak antiferromagnetic interactions between $S = {}^9/_2$ trinuclear units are operative. We can notice here that introducing an elusive interaction between terminal Ni^{2+} ions would not improve the situation as far as the very low temperature data are concerned. Taking into account the intermolecular effects in a mean-field approximation and minimizing *R* resulted in $J = 1.5$ cm^{-1}, $|D_{Ni}| = 0.74$ cm^{-1}, $g_{Mn} = 2.0$, $g_{Ni} = 2.10$, and $zJ' = -0.07$ cm^{-1}. As usually, the sign of D_{Ni} cannot be determined. Let us note that, if the local anisotropy of the Mn^{2+} ion is assumed to be negligibly small, D_{Ni} and $D_{9/2}$ are related through[1]

$$D_{9/2} = D_{Ni}/16 \quad (2)$$

The value of *J* will be taken as 1.4(1) cm^{-1}. The spectrum of the nine E(*S*,*S*′) low-lying states is shown in Figure 3; *S* and *S*′ stand for the quantum numbers associated with the total spin operator and the nickel spin operator, respectively. Each state is represented by an arrow whose length is proportional to the spin value *S*. One can notice that the spin state structure is regular; the spin *S* decreases monotonically as the energy increases.[1] The energy gap between highest and lowest low-lying states is then equal to 16.8 ± 1.2 cm^{-1}.

To confirm the nature of the ground state, the field dependence of the magnetization was measured at 2 K and up to 50 kOe. The results are compared to both the theoretical curve for an $S = {}^9/_2$ spin with a Zeeman factor $g_{9/2} = 2.04$ and the theoretical curve for isolated S_{Mn} and two S_{Ni} local spins with $g_{Mn} = 2$ and $g_{Ni} = 2.10$ in Figure 4. The g_{Mn} and g_{Ni} values are those deduced from the fitting of the $\chi_M T$ versus *T* curve (model II), and the $g_{9/2}$ value of the Zeeman factor associated with the ground state is related to the local Zeeman factors through[1]

$$g_{9/2} = (5g_{Mn} + 4g_{Ni})/9 \quad (3)$$

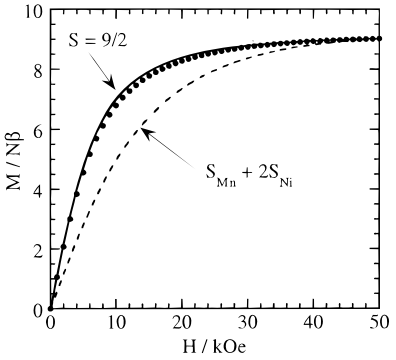

Figure 4. Field dependence of the magnetization at 2 K for $Mn(N_3)_4[Ni(en)_2NO_2]_2$ (●). These experimental data are compared to the theoretical curves expected for an $S = {}^9/_2$ state of the triad (—), and isolated $S_{Mn} + 2S_{Ni}$ spins (---) (see text).

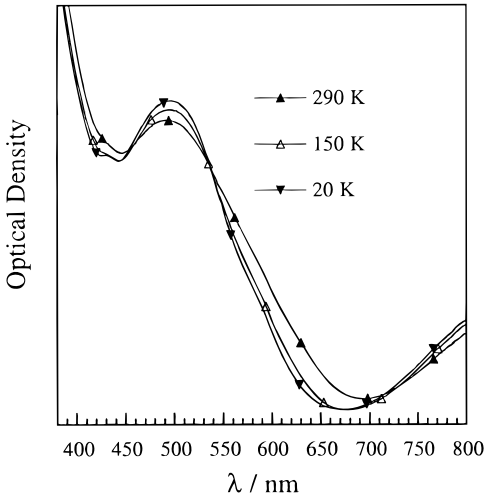

Figure 5. Absorption spectrum of $Mn(N_3)_4[Ni(en)_2NO_2]_2$ in a cellulose acetate pellet at room temperature, 150 K, and 20 K.

The experimental data are very slightly below the former curve and far from the latter. The slight difference between experimental data and the Brillouin function for an $S = {}^9/_2$ spin is due to the fact that at 2 K the population of the $S = {}^9/_2$ ground state is 0.898 (for $J = 1.4$ cm^{-1}); the first low-lying excited states of lower spin multiplicity are weakly populated.

The X-band powder EPR spectra of $Mn(N_3)_4[Ni(en)_2NO_2]_2$ were also investigated down to 4.2 K. At any temperature, the spectrum is very badly resolved and shows two features centered at $g = 2.00$ whose line widths are about 870 and 2020 Oe, respectively.

Optical Properties

The absorption spectrum of the title compound in a cellulose acetate pellet at room temperature shows a band centered at 11 700 cm^{-1} (855 nm) and an intense band centered at 20 121 cm^{-1} (497 nm) with a shoulder at 16 950 cm^{-1} (590 nm). At 20 K, this spectrum is almost unchanged, with a weak additional feature appearing at 23 150 cm^{-1} (432 nm). The spectra at three temperatures are compared in Figure 5.

The room-temperature spectrum is rather similar to that obtained for $Ni(NH_3)_4(NO_2)_2$,[19] and $Ni(en)_2(NO_2)_2$.[20] The low-energy bands correspond to the d−d transitions for Ni^{2+} in an octahedral environment (11 700 cm^{-1}, $^3A_{2g} \rightarrow {}^3T_{2g}$ (O_h); 16 950 cm^{-1}, $^3A_{2g} \rightarrow {}^3T_{1g}$ (O_h)). The band at 20 121 cm^{-1} is characteristic of Ni^{2+} compounds containing nitro ligands. It has been suggested that this transition was a weak $Ni^{2+} \rightarrow$ nitro charge-transfer transition.[21,22] It presumably corresponds to an $e_g(Ni^{2+}) \rightarrow \pi^*$(nitro) excitation involving orthogonal orbitals in the absence of vibronic coupling. The origin of the band at 23 150 cm^{-1} is unclear; it might be due to vibronic coupling.

It is worth pointing out that the Mn^{2+} spin-forbidden transitions activated by an exchange mechanism, if any, would be hidden by the band at 23 130 cm^{-1}, in contrast with what happens for the $Mn^{2+}Cu^{2+}$ species recently described.[23]

Discussion and Conclusion

From chemical intuitions and information arising from previous works, we succeeded in synthesizing a molecular species in which Mn^{2+} and Ni^{2+} ions are ferromagnetically coupled. Our approach was essentially based on the fact that the end-on azido and nitro−nitrito bridges were known to be ferromagnetic couplers. The compound described in this paper is the first in which two different metal ions are bridged by an azido group. The Mn^{2+}−Ni^{2+} interaction parameter in the title compound has much the same value as in the chain compound $MnNi(NO_2)_4(en)_2$ involving only a nitro−nitrito bridge.

The problem which remains unsolved concerns the mechanism of the ferromagnetic interaction, and even if we do not have any definitive answer to formulate, we wish to address this problem a bit further. What is obvious is that the stabilization of the high-spin triad state is not due to the orthogonality of the magnetic orbitals. Indeed, Mn^{2+} has the $3d^5$ electronic configuration, and at least one of the five singly occupied orbitals gives a nonzero overlap integral with the Ni^{2+} singly occupied orbitals, whatever the geometry of the bridging network may be.[1] On the other hand, there is a mechanism of ferromagnetic interaction which might be operative in the present case, namely the coupling between the ground configuration and some excited configurations in which an electron is transferred from a Ni^{2+} doubly occupied orbital (arising from the t_{2g} subset) to a Mn^{2+} singly occupied orbital. This mechanism, suggested for the first time by Goodenough,[24] was recently worked out in some details.[25] Of course, the nature of the bridges plays a key role in the stabilization of the $S = {}^9/_2$ triad state. In a forthcoming paper, we will explore the specificity of the end-on azido bridge in great detail, using the results of polarized neutron diffraction data and density functional calculations.

This paper represents a new example of molecular engineering of coupled systems.

Supporting Information Available: X-ray crystallographic files, in CIF format, available on the Internet only. Access information is given on any current masthead page.

IC9708531

(19) Hitchman, M. A.; Rowbottom, G. L. *Inorg. Chem.* **1982**, *21*, 823.
(20) Bertini, I.; Gatteschi, D.; Scozzafava, A. *Inorg. Chem.* **1976**, *15*, 203.
(21) Walker, I. M.; Lever, A. B. P.; MacCarthy, P. *Can. J. Chem.* **1980**, *58*, 823.
(22) Hitchman, M. A.; Rowbottom, G. L. *Coord. Chem. Rev.* **1982**, *42*, 55.
(23) Cador, O.; Mathonière, C.; Kahn, O. *Inorg. Chem.* **1997**, *36*, 1923.
(24) Goodenough, J. B. *Phys. Rev.* **1955**, *100*, 564; *J. Phys. Chem. Solids* **1958**, *6*, 287.
(25) Hotzelmann, H.; Wieghardt, K.; Flörke, U.; Haupt, H. J.; Weatherburn, D. C.; Bonvoisin, J.; Blondin, G.; Girerd, J. J. *J. Am. Chem. Soc.* **1992**, *114*, 1681.